Revision 1

NanoSIMS Pb/Pb dating of tranquillityite in high-Ti lunar basalts: Implications for the chronology of high-Ti volcanism on the Moon

Romain Tartèse[1], Mahesh Anand[1,2] and Thomas Delhaye[3]

[1]Planetary and Space Sciences, The Open University, Walton Hall, Milton Keynes, MK7 6AA, United Kingdom

[2]Department of Earth Sciences, The Natural History Museum, Cromwell Road, London, SW7 5BD, United Kingdom

[3]Plateforme ONIS/NanoSIMS, Université de Rennes 1, Campus de Beaulieu, 35042 Rennes Cedex, France

Abstract

In this study, we carried out Pb/Pb dating of tranquillityite in high-Ti mare basalts 10044, 75055 and 74255, using a Cameca NanoSIMS 50 at a spatial resolution of ~ 3 µm. The analyses yielded $^{207}Pb/^{206}Pb$ dates of 3722 ± 11 Ma for sample 10044, 3772 ± 9 Ma for sample 75055 and 3739 ± 10 Ma for sample 74255, at 95% confidence level. These dates are consistent with previously determined crystallization and emplacement ages of these samples using different radiogenic systems. These high-precision ages allow refinement of the timing of some of the high-Ti basaltic volcanism on the Moon. Crystallization ages of three different high-Ti basalt units, integrating these new Pb/Pb ages with previous Rb-Sr and Sm-Nd age determinations, are consistent with previous estimates but associated with uncertainties 3 to 5 times lower. In addition, the data obtained in this study confirm that tranquillityite contains very low amounts of initial common Pb and has a high Pb ionization efficiency, making it an excellent candidate for Pb/Pb dating by ion microprobe. The higher spatial resolution afforded by NanoSIMS 50 and the recent discovery of tranquillityite in several terrestrial mafic rocks opens up a new area of research allowing an independent and rapid age dating of basaltic rocks in polished sections.

Keywords: Ion probe; High-Ti mare basalts; NanoSIMS 50; Pb/Pb dating; Tranquillityite

Introduction

U-Th-Pb geochronology by ion microprobe was first carried out three decades ago by Andersen and Hinthorne (1972, 1973) to date phosphates and Zr-rich minerals from lunar samples. These pioneering studies demonstrated the potential of Secondary Ion Mass Spectrometry (SIMS) for *in-situ* geochronology, but the low mass resolution of the instrument used introduced some major limitations, notably related to isobaric interferences on the Pb isotopes. The development of the Sensitive High Resolution Ion Micro Probe (SHRIMP) permitted an efficient separation of isobaric interferences on the Pb isotopes (see the review of Compston and Clement 2006), which allowed precise U-Pb age dating of lunar zircons (Compston et al. 1984). Since these initial studies, *in-situ* U-Pb age dating of lunar samples has often been focused on zircons (e.g., Nemchin et al. 2012, and references therein), except for the SHRIMP U-Pb age dating of phosphates from lunar meteorites (Anand et al. 2003; Terada et al. 2005; 2007a, 2007b). In lunar samples, zircon occurs in several rock types such as anorthosite, troctolite, gabbro-norite, quartz-monzodiorite, granite and felsite (e.g., Nemchin et al., 2012), but is absent in basaltic rocks, in which Zr, as well as, U and Th, are commonly hosted by baddeleyite, zirconolite and tranquillityite.

Ion microprobe studies in terrestrial and extraterrestrial samples have shown that *in-situ* analysis of baddeleyite (Wingate and Compston 2000; Wingate et al. 1998; Chamberlain et al. 2010; Li et al. 2010; Schmitt et al. 2010; Rodionov et al. 2012), zirconolite (Rasmussen and Fletcher 2004; Rasmussen et al. 2008; Zhang et al. 2010; Wang et al. 2012), and tranquillityite (Rasmussen et al. 2008; 2012) can yield precise and accurate U-Pb and/or Pb/Pb ages. Particularly, the suitability of the NanoSIMS 50 for dating purposes has been demonstrated on zircon (Takahata et al. 2008; Yang et al. 2012), monazite (Sano et al., 2006), baddeleyite (Yang et al. 2012) and zirconolite (Stern et al. 2005). U-Pb age dating of these minerals are however still hampered by crystal orientation effects for baddeleyite (e.g., Wingate and Compston 2000) or the lack of reference zirconolite and tranquillityite for which U and Pb isotopic compositions have been determined by an independent method. Among these minerals, tranquillityite might be most suitable for U-Pb and Pb/Pb geochronology on account of 1) its very low initial common Pb and 2) its high Pb ionization efficiency; ~ 5 times that for zirconolite and an order of magnitude higher than zircon (Rasmussen et al. 2008). Tranquillityite is commonly found in mare basalts from all the Apollo landing sites and has also been described from KREEP basalts (see Rasmussen et al. 2008 and references therein). Moreover, it has recently been identified in dolerite rocks from six localities in Western Australia (Rasmussen et al. 2012), suggesting that it could be more widely present in terrestrial mafic rocks than previously recognized. However, tranquillityite commonly occurs as relatively thin grains (< 5 µm width) in lunar basalts, posing serious limitations for application of traditional geochronological techniques.

In this contribution, we present the results of Pb/Pb analyses carried out using the Cameca NanoSIMS 50 ion microprobe on tranquillityite grains occurring in high-Ti lunar basalts collected during Apollo 11 (10044) and Apollo 17 (75055 and 74255) missions. The Pb/Pb dates acquired in this study have been integrated into a review of previous age determinations for high-Ti mare basalts, allowing for a detailed discussion of the chronology of high-Ti mare volcanism at the Apollo 11 and 17 landing sites.

Samples

We have carried out Pb/Pb age dating of discrete tranquillityite grains from Apollo 11 sample 10044 and Apollo 17 samples 75055 and 74255. Sample 10044 is a coarse-grained porphyritic ilmenite basalt, with high-Ti and low-K contents (Schmitt et al. 1970; Beaty and Albee 1978a, 1978b). Rb-Sr and Ar/Ar age dating indicate a crystallization age of ~ 3.65 - 3.70 Ga (Papanastassiou et al. 1970; Turner 1970; Guggisberg et al. 1979), although Davis et al. (1971) reported an older Ar/Ar date of about 4.0 Ga. Sample 75055 is a fine- to medium-grained intergranular to subophitic ilmenite basalt (e.g., Dymek et al. 1975), with high-Ti and low-K contents (e.g., Rhodes et al. 1976). Its crystallization age has been determined using the Rb-Sr and Ar/Ar techniques at ~ 3.75 - 3.80 Ga (Huneke et al. 1973; Tatsumoto et al. 1973; Tera et al. 1974). Sample 74255 is a medium- to coarse-grained vesicular porphyritic basalt with abundant ilmenite (e.g., Dymek et al. 1975), with also high-Ti and low-K contents (e.g., Rhodes et al. 1976). Rb-Sr data gave an imprecise crystallization age of ~ 3.70 - 3.80 Ga (Murthy and Coscio 1976; Nyquist et al. 1976).

In samples 10044 and 75055, tranquillityite, with an ideal formula $[Fe_8^{2+}(Zr,Y)_2Ti_3Si_3O_{24}]$, commonly occurs as intergrowths of laths 20 to 50 μm long that crystallized in late-stage mesostasis areas and in voids in plagioclase. Tranquillityite crystals were relatively smaller in size in sample 74255. Tranquillityite composition is similar in samples 10044 and 75055, roughly comprising of 14 - 15 wt.% SiO_2, 43 - 44 wt.% FeO and ~ 16 wt.% ZrO_2, with TiO_2 content slightly higher in 75055 than in 10044 (Table 1). Tranquillityite in 74255 differs in terms of having higher SiO_2 and lower FeO contents compared to those in samples 10044 and 75055 (Table 1). These chemical compositions are consistent with those reported from other high-Ti mare basalts, but differ considerably from terrestrial tranquillityite (Table 1 and Fig. 1).

Analytical setup

Polished thin sections 10044,645, 75055,49 and 74255,48 were obtained from the Lunar Sample Curation facility at the Johnson Space Centre (NASA). Back-scattered electron (BSE) images and X-ray maps of the entire polished sections were acquired using a Quanta 3D dual beam Focused Ion Beam (FIB) Secondary Electron Microscope (SEM) at the Open University, UK, fitted with an Oxford Instruments INCA energy dispersive X-ray detector.

For this purpose, sections were carbon coated and examined with an electron beam current of 0.6 nA at an accelerating voltage of 20 kV. We used the whole-section X-ray maps of Zr to locate Zr-bearing minerals, and then acquired high magnification BSE images of areas containing these Zr-bearing minerals. X-ray spectra were then acquired for 60 seconds to get quantitative chemical compositions of tranquillityite grains (see Tables S2 and S3 in the Supplementary Material).

The Pb/Pb analyses were carried out using the Cameca NanoSIMS 50 installed at the University of Rennes 1, France. The NanoSIMS is a scanning ion microscope equipped with a double-focusing mass analyzer allowing high mass and spatial resolution. The NanoSIMS differs from other ion microscopes by its co-axial design that comprises a normal primary ion beam and a co-axial secondary ion extraction, optimizing simultaneously the objective lens performance and collection of secondary ions. The NanoSIMS design also reduces the distance between the sample and the objective, allowing for a smaller spot size for a given probe current compared to other ion microscopes. General descriptions of the instrument and of the tuning specific to Pb/Pb analyses can be found in Slodzian et al. (1992) and in Stern et al. (2005), respectively.

In the NanoSIMS 50, the primary column integrates a duoplasmatron ion source in which the negative oxygen ions are accelerated through a potential of - 8 kV, passed through a Wien mass filter for isolation of $^{16}O^-$ ions, which are then focused to the target held at a positive potential of + 8 kV, resulting in a total impact energy of 16 keV. For tranquillityite analyses, the O^- beam was optimized using apertures D0-1 and D1-2, resulting in a current of ~ 120 - 140 pA on the sample surface. Each spot size on the sample surface was ~ 3.5 μm × 2.5 μm (Fig. 2), corresponding to a beam density of ~ 15 pA.μm^{-2}, which is similar to the value reported by Stern et al. (2005). During the analytical sessions, the vacuum in the analysis chamber remained constant at ~ 8 × 10^{-10} torr.

Secondary ions excavated from the sample were extracted by the co-axial immersion lens and focused onto a fixed-width analyzer entrance slit (ES). In this study, we used ES-3 (30 μm), which cuts about 60% of the secondary ions relative to the full transmission without slits. An additional 10% of the secondary ions were lost at the aperture slit (AS-1). No energy slit was used. The net relative transmission at high resolution was therefore ~ 35%. With this setup, we achieved a mass resolving power of ~ 5000 (Cameca definition, equivalent to a mass resolution of ~ 3500), sufficient to isolate the major $^{178\text{-}179}Hf^{28}Si$ interferences on the ^{206}Pb and ^{207}Pb peaks in tranquillityite. The mass spectrometer of the NanoSIMS 50 installed in Rennes comprises of 5 detectors equipped with electron multipliers (EM), allowing for 5 species to be simultaneously counted under a static magnetic field. Although for Zr-bearing minerals it is possible to simultaneously measure Pb, UO and UO_2, it is not possible to measure ^{204}Pb, ^{206}Pb and ^{207}Pb at the same time because the dispersion distance between the Pb isotopes at the focal plane is less than the minimum separation of detectors. The Pb isotopes were therefore analyzed in the magnetic peak-switching mode on the detector EM#4. Between each analysis, the magnet field settings for the Pb peak positions were precisely determined manually and the ^{206}Pb peak was used to set the automatic centering procedure.

Before analysis, the probe was rastered over a 6 μm × 6 μm area for ~ 5 min to remove any potential surface contamination. For analysis, the scanning mode of the probe was switched off and the magnetic field was cyclically switched to measure ^{204}Pb, ^{206}Pb and ^{207}Pb in an up-mass sequence. Automatic centering was performed on the ^{206}Pb peak at the beginning of each analysis and repeated three times during a run. Counting times were set to 4 s for ^{206}Pb and 10 s for ^{204}Pb and ^{207}Pb, with a 2 s waiting time between each isotopic measurement, resulting in a total analysis time of about 30 minutes. The EM background is set to 0 in the NanoSIMS setup, and it was not further monitored in this study. Raw data were corrected for EM dead time of 44 ns by the NanoSIMS software. The secondary ion signals were processed using the NanoSIMS DataEditor software developed by Frank Gyngard (Washington University, St Louis, USA), and isotope ratios were calculated from total counts. Final date calculations were carried out using the Isoplot 3.7 add-in for Excel (Ludwig 2008). No corrections were applied for instrumental mass fractionation. Stern and Amelin (2003) discussed up to 0.2%/amu fractionation of Pb isotopes during SHRIMP analyses, which tends to lower the measured $^{207}Pb/^{206}Pb$ ratio. On the other hand, the presence of unresolved hydride ^{206}PbH mixed with ^{207}Pb has an opposite effect, raising the $^{207}Pb/^{206}Pb$ ratio. Thus, mass fractionation and hydride interferences are probably cancelling effects of each other (e.g. Ireland and Williams 2003). Consistently, instrumental mass fractionation for Pb isotopes has been shown to be negligible for NanoSIMS measurements in mono-collection mode (Stern et al. 2005), even with a static probe (Yang et al. 2012).

Results

Before analysis, we acquired a 128 pixels × 128 pixels ion image of the 45 µm × 45 µm area enclosing tranquillityite #14 and the associated baddeleyite in sample 10044. Secondary species ^{47}Ti, ^{91}Zr, ^{206}Pb and $^{238}U^{16}O$ were simultaneously monitored during 5 min 33 s, with a dwell time of 20 ms/px. The data were processed offline using the L'Image software package (L.R. Nittler, Carnegie Institution, USA) to produce the maps displayed in Figure 3. In agreement with their general chemical compositions, images show that tranquillityite is richer in Ti and poorer in Zr than baddeleyite. Baddeleyite also appears richer in ^{238}U than tranquillityite, whereas count rates for ^{206}Pb is higher in tranquillityite than in baddeleyite. This illustrates that Pb is more efficiently ionized in tranquillityite than in baddeleyite. A high Pb ionization efficiency in tranquillityite is consistent with the observation of Rasmussen et al. (2008), who found Pb ionization efficiency for tranquillityite about 5 times that for zirconolite during their SHRIMP analyses.

The Pb isotopic compositions of tranquillityite in the three mare basalt samples are given in Table 2. The common Pb content of tranquillityites analyzed in this study is very low, as indicated by measured $^{204}Pb/^{206}Pb$ ratios of lower than 0.0002 (Table 2). As a result, it precludes calculation of $^{207}Pb/^{206}Pb$ vs. $^{204}Pb/^{206}Pb$ isochron ages due to the low dispersion in the $^{204}Pb/^{206}Pb$ ratios (Fig. 4). Arrows pointing to the Pb isotopic composition of two possible contaminants are depicted in the $^{207}Pb/^{206}Pb$ vs. $^{204}Pb/^{206}Pb$ mixing diagrams (Fig. 4). When the measured ratios are highly radiogenic, which is the case here for lunar tranquillityites, any common Pb is likely to be mainly associated with polishing compounds and/or the conductive coating (e.g., Williams 1998). The Broken Hill galena Pb composition ($^{204}Pb/^{206}Pb = 0.0626$, $^{207}Pb/^{206}Pb = 0.961$; Sangster et al. 2000) has been used to model this laboratory contamination, which is depicted by a grey arrow in Figure 4. The second arrow points towards an estimated lunar initial Pb. For this purpose, the values of Rasmussen et al. (2008) ($^{207}Pb/^{206}Pb = 1.43$ and $^{204}Pb/^{206}Pb = 0.0074$) have been used. These authors carried out several Pb/Pb analyses in K-feldspar and other matrix minerals in the high-Ti basalt 10047, and found that such a composition, computed for a single-stage evolution from the Canyon Diablo troilite primordial isotopic composition until 3.7 Ga and a μ value of 500, matches well their measured data. In the three samples analyzed in this study, the majority of the Pb isotope ratios could be interpreted as mixing between a ^{204}Pb-free $^{207}Pb/^{206}Pb$ ratio, corresponding to the average of the measured $^{207}Pb/^{206}Pb$ ratios, and a very small component of Pb introduced by laboratory contamination (Fig. 4). The fraction of ^{206}Pb (f_{206}) comprising unradiogenic Pb, calculated using the measured $^{204}Pb/^{206}Pb$ and the Broken Hill Pb composition, never exceeds 0.3% (Table 2). As a result, the dates calculated using the measured $^{207}Pb/^{206}Pb$ ratios and those corrected for unradiogenic Pb differ by a maximum of 0.2%. Uncertainties in age determinations are thus largely dominated by counting uncertainties, which is the reason why we used the measured $^{207}Pb/^{206}Pb$ ratios to calculate individual dates.

In Apollo 11 sample 10044, the 9 analyses carried out on 5 different grains define a weighted mean $^{207}Pb/^{206}Pb$ date of 3722 ± 11 Ma (95% confidence level), with a MSWD of 1.3 (Fig. 4a). In Apollo 17 sample 75055, 12 analyses carried out on 5 different tranquillityite grains yield a weighted mean $^{207}Pb/^{206}Pb$ date of 3772 ± 9 Ma (MSWD = 1.9; 95% confidence level; Fig. 4b). In sample 74255, 7 analyses carried out on 4 grains display more scatter compared to other two samples. Excluding the two outliers (Trq4#1 and Trq18#1; Fig. 4c), the remaining 5 analyses, carried out on 3 grains, define a weighted mean $^{207}Pb/^{206}Pb$ date of 3739 ± 10 Ma (MSWD = 1.9; 95% confidence level, Fig. 4c). One analysis was also carried out on a baddeleyite grain associated with tranquillityite #14 in sample 10044 (Figs. 2 and 3). The measured $^{204}Pb/^{206}Pb$ and $^{207}Pb/^{206}Pb$ ratios are slightly higher and lower than in tranquillityite, respectively. These ratios are also associated with higher uncertainties (Table 2), due to lower count rates for both ^{206}Pb and ^{207}Pb in baddeleyite (about an order of magnitude lower than in tranquillityite). Nevertheless, the calculated $^{207}Pb/^{206}Pb$ date of 3682 ± 90 Ma is consistent within errors of the weighted mean $^{207}Pb/^{206}Pb$ date calculated from tranquillityite analyses.

As an external control, analyses were also carried out on a chip of the well characterized Phalaborwa baddeleyite standard (details are given in the Supplementary Material). The 15 individual $^{207}Pb/^{206}Pb$ analyses define a weighted mean $^{207}Pb/^{206}Pb$ date of 2065 ± 15 Ma (Supplementary Fig. S1 and Table S1), which is consistent with the $^{207}Pb/^{206}Pb$ crystallization ages of ~ 2060 Ma determined for Phalaborwa baddeleyite by ID-TIMS (Reischmann 1995; Heaman 2009).

Discussion

Accuracy of the tranquillityite Pb/Pb dates

Since Pb/Pb dating is not amenable to the concordance test afforded by U-Pb dating, it is imperative to ensure that the tranquillityite Pb/Pb data accurately date the crystallization ages of the parental magmas. Indeed, these small tranquillityite grains might have been affected by diffusive loss of Pb after crystallization, for example, as a result of impact processes. Moreover, the closure temperature for diffusion of Pb isotopes in tranquillityite is currently unknown. Rasmussen et al. (2008) discussed the issue of possible disturbance of the Pb isotopic systematics in Zr-rich minerals in Apollo 11 sample 10047. Based notably on the comparison between zirconolite and tranquillityite Pb/Pb ages determined in sample 10047, these authors argued that $^{207}Pb/^{206}Pb$ systematics in these two minerals provided an accurate and precise chronometer, and that dating lunar samples using these minerals appears to be more limited by the $^{207}Pb/^{206}Pb$ data obtained on reference materials than by data obtained on the minerals themselves. As we only dated tranquillityite, we cannot evaluate consistency between dates given by tranquillityite and by another mineral. However, the obtained Pb/Pb ages can be compared with previous age determinations carried out on the studied samples using other chronometers. In the following, all previously published Rb-Sr and Sm-Nd ages have been recalculated using the Isoplot add-in for Excel (Ludwig 2008) to ensure a thorough propagation of uncertainties. Moreover, the new decay constant for ^{87}Rb of 1.3968×10^{-11} yr^{-1} (Rotenberg et al. 2012) has been used to recalculate Rb-Sr isochron ages.

Sample 10044 was first dated soon after the Apollo 11 astronauts brought it back to the Earth. Papanastassiou et al. (1970) determined a Rb-Sr isochron date of 3694 ± 68 Ma (whole-rock and mineral fractions, excluding their Pyroxene A fraction; Table 3). Turner (1970) and Guggisberg et al. (1979) used the Ar/Ar chronometer and obtained whole-rock plateau dates of 3.73 ± 0.05 Ga and 3.71 ± 0.04 Ga, respectively. The tranquillityite Pb/Pb date of 3722 ± 11 Ma obtained in this study is in good agreement with these previous Rb-Sr and Ar/Ar age determinations. Moreover, our tranquillityite Pb/Pb date of 3722 ± 11 Ma is consistent with the precise $^{207}Pb/^{206}Pb$ date of 3710 ± 5 Ma determined on sample 10047 by Rasmussen et al. (2008), which is petrologically identical to sample 10044 and probably came from the same lava flow (Beaty and Albee 1978b). The Pb/Pb date of 3772 ± 9 Ma determined on tranquillityite in sample 75055 is consistent with the Rb-Sr isochron date of 3752 ± 60 Ma determined by Tera et al. (1974) (Table 3). It is also consistent with the well-defined plateau Ar/Ar date of 3.78 ± 0.04 Ga obtained on a plagioclase separate by Huneke et al. (1973). In sample 74255, $^{207}Pb/^{206}Pb$ ratios measured in tranquillityite grains display more scatter (Fig. 4). Two previous studies determined whole-rock mineral Rb-Sr isochron dates of 3751 ± 77 Ma (Nyquist et al. 1976) and 3694 ± 140 Ma (Murthy and Coscio 1976), respectively. Combination of these two dataset yields a Rb-Sr isochron date of 3750 ± 120 Ma (Table 3). Considering the very large uncertainty associated with the date determined by Murthy and Coscio (1976), this date, apart from being consistent with our tranquillityite Pb/Pb date of 3739 ± 10 Ma, is too imprecise to be useful in the present context of age comparisons. The large uncertainties associated with Rb-Sr isochron dates and the presence of two outliers in our Pb isotopic data may indicate that this sample experienced some geological disturbance.

Chronology of high-Ti volcanism at Apollo 11 and 17 landing sites

Mare-basalts returned from the Apollo 11 landing site have been classified in five different types, namely A, B1, B2, B3 and D (Beaty and Albee 1978a; Beaty et al. 1979; Ma et al. 1980; Rhodes and Blanchard 1980). The crystallization ages of these mare-basalts span the range from ~ 3.60 to 3.90 Ga (e.g., Papanastassiou et al. 1977; Guggisberg et al. 1979). Previous Rb-Sr and Sm-Nd age determinations yielded a weighted mean crystallization age of

3695 ± 50 Ma for mare basalts from the B1 type. The new Pb/Pb dates obtained in this study and by Rasmussen et al. (2008) provide a more precise crystallization age of 3711 ± 4 Ma for basalts of the Apollo 11 B1 type (Fig. 5 and Table 3). Published Rb-Sr and Sm-Nd dates have been used to calculate the best estimates of the crystallization ages two other Apollo 11 types: the type B2 basalts are the oldest, with a crystallization age of 3852 ± 65 Ma, whereas type A basalts are the youngest with a well-defined crystallization age of 3597 ± 20 Ma (Fig. 5). These crystallization ages compare well with those summarized in previous synthesis (e.g., Jerde et al. 1994; Stöffler and Ryder 2001, and references therein), except for type B2 basalts that appears to be ~ 50 Ma older than the age considered by Stöffler and Ryder (2001). However, due to a relatively large uncertainty associated with the age determination of type B2 basalts, the exact timing of Apollo 11 type B2 volcanism remains uncertain. For future work, it is important to better constrain the crystallization ages of type B2 basalts as their ages have been used as an important unit for crater retention age determinations (e.g., Stöffler and Ryder 2001).

At the Apollo 17 landing site, basalts have been grouped into three types A, B and C based on their whole-rock chemical compositions (Rhodes et al. 1976). Neal et al. (1990) further divided type B basalts into groups B1 and B2. Sample 75055 belongs to the type A. Rb-Sr and Sm-Nd dates obtained on six samples from Apollo 17 type A basalts (Table 3) define a weighted mean date of 3769 ± 30 Ma, which is identical to the Pb/Pb date of 3772 ± 9 Ma obtained on tranquillityite in sample 75055. Integrating this date with previous determinations yield a weighted mean date of 3772 ± 9 Ma (Fig. 5), which we confidently interpret as the crystallization age of the Apollo 17 type A lava flow. This suggests that Apollo 17 type A lavas might have erupted ~ 20 Ma earlier than estimated previously (e.g. Paces et al. 1991; Stöffler and Ryder 2001). Sample 74255 belongs to the rare Apollo 17 Type C basalts, sampled at station 4 near Shorty crater. The three previous Rb-Sr age determinations carried out on sample 74255 and 74275 (Table 3) yielded an imprecise weighted mean date of 3755 ± 61 Ma, which is within error of the Pb/Pb tranquillityite date of 3739 ± 10 Ma. Based on the broad consistency between Rb-Sr age determinations and the Pb/Pb tranquillityite date obtained in this study on sample 74255, we propose that the crystallization age of the Apollo 17 type C lava flow is 3739 Ma ± 10 Ma. Our Pb/Pb crystallization age obtained on tranquillityite in type C sample 74255 provides a better constraint on the eruption age of this type, which was previously loosely constrained at 3750 ± 70 Ma (Stöffler and Ryder 2001, and references therein). However, additional age determinations on some other Apollo 17 type C basalts are desirable to firmly establish this crystallization age. Apollo 17 types A and C basalts have different crystallization ages of ~ 3772 Ma and ~ 3739 Ma, respectively. Eruption ages of these two types of lavas are important as they also serve as age constraints for crater retention ages (Stöffler and Ryder 2001, and references therein). Finally, published Rb-Sr and Sm-Nd age determinations suggest that Apollo 17 type B basalts might have been emplaced at 3719 ± 44 Ma. Unfortunately, the uncertainty on this age is fairly large and new age determinations should be carried out on Apollo 17 type B basalts.

Figure 5 shows that Apollo 11 type B1 and Apollo 17 type B units have similar crystallization ages, suggesting that they could represent a unique and very widespread volcanic event. However, some of their whole-rock geochemical characteristics indicate that they constituted two different lava flows (Fig. 6). Nevertheless, their similarities in ages imply widespread volcanism on the Moon at the same time.

Implications for Pb/Pb age dating with the NanoSIMS

The Pb/Pb dates obtained on tranquillityites from three Apollo 11 and 17 high-Ti mare basalts are consistent with previous age determinations carried out using other radiogenic systems. Hence, we consider that these Pb/Pb dates are reliable and provide accurate crystallization ages. Provision of a suitable tranquillityite standard for U-Pb dating will help further confirm and refine the crystallization ages of mare-basalts containing tranquillityite. Tranquillityite, with its low initial Pb content and its high Pb ionization efficiency, would constitute an excellent reference material, allowing for the use of even smaller primary current and thus smaller spot sizes. As tranquillityite has now been identified in several terrestrial dolerite samples (Rasmussen et al. 2012), in some cases in large amounts (more than 100 individual crystals in some polished thin sections, as reported by Rasmussen et al. 2012), it may be possible to consider separating these crystals from large samples and use them as reference materials. It would require ID-TIMS analyses of both the Pb and the U isotopes, and provided that they are homogeneous, would constitute a good reference material.

Conclusion

The Pb/Pb crystallization ages determined on tranquillityite in this study indicate that high-Ti mare basalts 10044, 75055 and 74255 were emplaced on the lunar surface at 3722 ± 11 Ma, 3772 ± 9 Ma and 3739 ± 10 Ma, respectively. These ages are associated with a precision better than 0.3% at the 95% confidence level, for a beam size of ~ 2-3 µm, confirming the suitability of tranquillityite for Pb/Pb dating. These ages are also consistent with crystallization ages determined previously using different chronometers, but provide tighter constraints on the timing of eruption of three different types of high-Ti mare basalts. Additionally, our new high-precision Pb/Pb crystallization ages obtained on tranquillityite seem to indicate concurrent mafic volcanic activity at ~ 3.71 Ga on the lunar surface, represented by the Apollo 11 and Apollo 17 landing sites.

The small spatial resolution achieved in our dating protocol with the NanoSIMS 50 ion probe and the widespread occurrence of tranquillityite grains in mare basalts will allow better age constraints to be placed on different basaltic units sampled during the Apollo missions. This will ultimately lead to a better adjustment of the lunar calibration curve used for crater counting studies, which underpins all the ages estimated for other planetary bodies in the inner solar system.

Acknowledgments

We would like to acknowledge the support of the Science and Technology Facilities Council (STFC) for funding this research (Grant no. ST/I001298/1 to MA). We also thank NASA CAPTEM for allocation of lunar samples, Diane Johnson for her help with SEM analysis, and Marc Poujol for proofreading the manuscript. Critical and constructive comments made by Trevor Ireland and an anonymous reviewer helped significantly improve the manuscript. Finally, we thank the FEDER, the Région Bretagne, the Conseil Général d'Ille-et-Vilaine and Rennes Métropole for financial support of the imaging platform ONIS (GIS Europia).

References

Anand, M., Taylor, L.A, Neal, C.R., Snyder, G.A., Patchen, A., Sano, Y., and Terada, K. (2003) Petrogenesis of lunar meteorite EET 96008. Geochimica et Cosmochimica Acta, 67, 3499-3518.

Andersen, C.A. and Hinthorne, J.R. (1972) U, Th, Pb and REE abundances and $^{207}Pb/^{206}Pb$ ages of individual minerals in returned lunar material by ion microprobe mass analysis. Earth and Planetary Science Letters, 14, 195-200.

Andersen, C.A. and Hinthorne, J.R. (1973) $^{207}Pb/^{206}Pb$ ages of individual mineral phases in Luna 20 material by ion microprobe mass analysis. Geochimica et Cosmochimica Acta, 37, 745-754.

Beaty, D.W. and Albee, A.L. (1978a) Comparative petrology and possible genetic relations among the Apollo 11 basalts. 9th Lunar and Planetary Science Conference, 359-463.

Beaty, D.W. and Albee, A.L. (1978b) A textural, modal and chemical classification of the Apollo 11 low-K basalts. Lunar and Planetary Science, IX, 61-63.

Beaty, D.W., Hill, S.M.R., and Albee, A.L. (1979) Petrology of a new rock type from Apollo 11: Group D basalts. Lunar and Planetary Science, X, 89-91.

Chamberlain, K.R., Schmitt, A.K., Swapp, S.M., Harrison, T.M., Swoboda-Colberg, N., Bleeker, W., Peterson, T.D., Jefferson, C.W., and Khudoley, A.K. (2010) In situ U-Pb SIMS (IN-SIMS) micro-baddeleyite dating of mafic rocks: Method with examples. Precambrian Research, 183, 379-387.

Compston, W. and Clement, S.W.J. (2006) The geological microprobe: The first 25 years of dating zircons. Applied Surface Science, 252, 7089-7095.

Compston, W., Williams, I.S., and Meyer, C. (1984) U-Pb geochronology of zircons from lunar breccia 73217 using a sensitive high-resolution ion microprobe. Journal of Geophysical Research, 89, B525-B534, doi: 10.1029/JB089iS02p0B525.

Davis, P.K., Lewis, R.S., and Reynolds, J.H. (1971) Stepwise heating analysis of rare gases from pile-irradiated rocks 10044 and 10057. 2nd Lunar Science Conference, 2, 1693-1703.

Dymek, R.F., Albee, A.L., and Chodos, A.A. (1975) Comparative mineralogy and petrology of Apollo 17 mare basalts: Samples 70215, 71055, 74255, and 75055. 6th Lunar Science Conference, 1, 49-77.

Evensen, N.M., Murthy, V.R., and Coscio M.R. (1973) Rb-Sr ages of some mare basalts and the isotopic and trace element systematics in lunar fines. 4th Lunar Science Conference, 2, 1707-1724.

Guggisberg, S., Eberhardt, P., Geiss, J., Grögler, N., Stettler, A., Brown, G.M., and Peckett, A. (1979) Classification of the Apollo-11 mare basalts according to Ar^{39}-Ar^{40} ages and petrological properties. 10th Lunar and Planetary Science Conference, 1-39.

Heaman, L.M. (2009) The application of U-Pb geochronology to mafic, ultramafic and alkaline rocks: An evaluation of three mineral standards. Chemical Geology, 261, 43-52.

Huneke, J.C., Jessberger, E.K., Podosek, F.A., and Wasserburg, G.J. (1973) $^{40}Ar/^{39}Ar$ measurements in Apollo 16 and 17 samples and the chronology of metamorphic and volcanic activity in the Taurus Littrow region. 4th Lunar Science Conference, 1725-1756.

Ireland, T.R. and Williams, I.S. (2003) Considerations in zircon geochronology by SIMS. Reviews in Mineralogy and Geochemistry, 53, 215-241.

Jerde, E.A., Snyder, G.A., Taylor, L.A., Liu, Y.G., and Schmitt, R.A. (1994) The origin and evolution of lunar high-Ti basalts: Periodic melting of a single source at Mare Tranquillitatis. Geochimica et Cosmochimica Acta, 58, 515-527.

Li, Q.L., Li, X.H., Liu, Y., Tang, G.Q., Yang, J.H., and Zhu, W.G. (2010) Precise U-Pb and Pb/Pb dating of Phanerozoic baddeleyite by SIMS with oxygen flooding technique. Journal of Analytical Atomic Spectrometry, 25, 1107-1113.

Lovering, J.F., Wark, D.A., Reid, A.F., Ware, N.G., Keil, K., Prinz, M., Bunch, T.E., El Goresy, A., Ramdohr, P., Brown, G.M., Peckett, A., Phillips, R., Cameron, E.N., Douglas, J.A.V., and Plant, A.G. (1971) Tranquillityite: A new silicate mineral from Apollo 11 and Apollo 12 basaltic rocks. 2nd Lunar Science Conference, 1, 39-45.

Ludwig, K.R. (2008) Isoplot/Ex Version 3.70: A Geochronological Toolkit for Microsoft Excel. Berkeley Geochronology Center, Special Publication 4, 73 pp.

Lugmair, G.W., Scheinin, N.B., and Marti, K. (1975) Sm-Nd age and history of Apollo 17 basalt 75075: Evidence for early differentiation of the lunar interior. 6th Lunar Science Conference, 1419-1429.

Ma, M.S., Schmitt, R.A., Beaty, D.W., and Albee, A.L. (1980) The petrology and chemistry of basaltic fragments from the Apollo 11 soil: Drive tubes 10004 and 10005. 11th Lunar and Planetary Science Conference, 37-47.

Meyer, H.O.A. and Boctor, N.Z. (1974) Opaque mineralogy: Apollo 17, rock 75035. 5th Lunar Science Conference, 1, 707-716.

Murthy, V.R. and Coscio, C. (1976) Rb-Sr ages and isotopic systematics of some Serenitatis mare basalts. 7th Lunar Science Conference, 2, 1529-1544.

Murthy, V.R. and Coscio, C. (1977) Rb-Sr isotopic systematics and initial Sr considerations for some lunar samples. 8th Lunar Science Conference, 706-708.

Neal, C.R., Taylor, L.A., Patchen, A.D., Hughes, S.S., and Schmitt, R.A. (1990) The significance of fractional crystallization in the petrogenesis of Apollo 17 Type A and B high-Ti basalts. Geochimica et Cosmochimica Acta, 54, 1817-1833.

Nemchin, A.A., Grange, M.L., Pidgeon, R.T., and Meyer, C. (2012) Lunar zirconology. Australian Journal of Earth Science, 59, 277-290.

Nyquist, L.E., Bansal, B.M., Wiesmann, H., and Jahn B.M. (1974) Taurus-Littrow chronology: some constraints on early lunar crustal development. 5th Lunar Science Conference, 2, 1515-1539.

Nyquist, L.E., Bansal, B.M., and Wiesmann H. (1975) Rb- Sr ages and initial $^{87}Sr/^{86}Sr$ for Apollo 17 basalts and KREEP basalt 15386. 6th Lunar Science Conference, 1445-1465.

Nyquist, L.E., Bansal, B.M., and Wiesmann, H. (1976) Sr isotopic constraints on the petrogenesis of Apollo 17 mare basalts. 7th Lunar Science Conference, 2, 1507-1528.

Nyquist, L.E., Shih, C.Y., Wooden, J.L., Bansal, B.M., and Wiesmann H. (1979) The Sr and Nd isotopic record of Apollo 12 basalts: Implications for lunar geochemical evolution. 10th Lunar and Planetary Science Conference, 77-114.

Paces, J.B., Nakai, S., Neal, C.R., Taylor, L.A., Halliday, A.N., and Lee, D.C. (1991) A strontium and neodymium isotopic study of Apollo 17 high-Ti mare basalts: Resolution of ages, evolution of magmas, and origins of source heterogeneities. Geochimica et Cosmochimica Acta, 55, 2025-2043.

Papanastassiou, D.A. and Wasserburg, G.J. (1971) Lunar chronology and evolution from Rb-Sr studies of Apollo 11 and 12 samples. Earth and Planetary Science Letters, 11, 37-62.

Papanastassiou, D.A. and Wasserburg, G.J. (1975) A Rb-Sr study of Apollo 17 boulder 3: Dunite clast, microclasts, and matrix. 6th Lunar Science Conference, 631-633.

Papanastassiou, D.A., Wasserburg, G.J., and Burnett, D.S. (1970) Rb-Sr ages of lunar rocks from the Sea of Tranquillity. Earth and Planetary Science Letters, 8, 1-19.

Papanastassiou, D.A., DePaolo, D.J., and Wasserburg, G.J. (1977) Rb-Sr and Sm-Nd chronology and genealogy of mare basalts from the Sea of Tranquility. 8th Lunar Science Conference, 1639-1672.

Rasmussen, B. and Fletcher, I.R. (2004) Zirconolite: A new U-Pb chronometer for mafic igneous rocks. Geology, 32, 785-788.

Rasmussen, B., Fletcher, I.R., and Muhling, J.R. (2008) Pb/Pb geochronology, petrography and chemistry of Zr-rich accessory minerals (zirconolite, tranquillityite and baddeleyite) in mare basalt 10047. Geochimica et Cosmochimica Acta, 72, 5799-5818.

Rasmussen, B., Fletcher, I.R., Gregory, C.J., Muhling, J.R., and Suvorova, A.A. (2012) Tranquillityite: The last lunar mineral comes down to Earth. Geology, 40, 83-86.

Reischmann, T. (1995) Precise U/Pb age determination with baddeleyite (ZrO_2), a case study from the Phalaborwa igneous complex, South Africa. South African Journal of Geology, 98, 1-4.

Rhodes, J.M., Hubbard, N.J., Wiesmann, H., Rodgers, K.V., Brannon, J.C., and Bansal, B.M. (1976) Chemistry, classification, and petrogenesis of Apollo 17 mare basalts. 7th Lunar Science Conference, 2, 1467-1489.

Rhodes, J.M. and Blanchard, D.P. (1980) Chemistry of Apollo 11 low-K mare basalts. 11th Lunar and Planetary Science Conference, 49-66.

Rodionov, N.V., Belyatsky, B.V., Antonov, A.V., Kapitonov, I.N., Sergeev, S.A. (2012) Comparative in-situ U-Th-Pb geochronology and trace element composition of baddeleyite and low-U zircon from carbonatites of the Palaeozoic Kovdor alkaline-ultramafic complex, Kola Peninsula, Russia. Gondwana Research, 21, 728-744.

Rotenberg, E., Davis, D.W., Amelin, Y., Ghosh, S., and Bergquist, B.A. (2012) Determination of the decay-constant of ^{87}Rb by laboratory accumulation of ^{87}Sr. Geochimica et Cosmochimica Acta, 85, 41-57.

Sangster, D.F., Outridge, P.M., and Davis, W.J. (2000) Stable lead isotope characteristics of lead ore deposits of environmental significance. Environmental Reviews, 8, 115-147.

Sano, Y., Takahata, N., Tsutsumi, Y., and Miyamoto, T. (2006) Ion microprobe U-Pb dating of monazite with about five micrometer spatial resolution. Geochemical Journal, 40, 597-608.

Schmitt, A.K., Chamberlain, K.R., Swapp, S.M., and Harrison, T.M. (2010) In situ U-Pb dating of micro-baddeleyite by secondary ion mass spectrometry. Chemical Geology, 269, 386-395.

Schmitt, H.H., Lofgren, G., Swann, G.A., and Simmons, G. (1970) The Apollo 11 samples: Introduction. Apollo 11 Lunar Science Conference, 1-54.

Simpson, P.R. and Bowie, S.H.U. (1971) Opaque phases in Apollo 12 samples. 2nd Lunar Science Conference, 1, 207-218.

Slodzian, G., Daigne, B., Girard, F., Boust, F., and Hillion, F. (1992) Scanning secondary ion analytical microscopy with parallel detection. Biology of the Cell, 74, 43-50.

Snyder, G.A., Lee, D.C., Taylor, L.A., Halliday, A.N., and Jerde, E.A. (1994) Evolution of the upper mantle of the Earth's Moon: Neodymium and strontium isotopic constraints from high-Ti mare basalts. Geochimica et Cosmochimica Acta, 58, 4795-4808.

Stern, R.A. and Amelin, Y. (2003) Assessment of errors in SIMS zircon U-Pb geochronology using a natural zircon standard and NIST SRM 610 glass. Chemical Geology, 197, 111-142.

Stern, R.A., Fletcher, I.R., Rasmussen, B., McNaughton, N.J., and Griffin, B.J. (2005) Ion microprobe (NanoSIMS 50) Pb-isotope geochronology at < 5 µm scale. International Journal of Mass Spectrometry, 244, 125-134.

Stöffler, D. and Ryder, G. (2001) Stratigraphy and isotope ages of lunar geologic units: Chronological standard for the inner solar system. Space Science Reviews, 96, 9-54.

Takahata, N., Tsutsumi, Y., and Sano, Y. (2008) Ion microprobe U-Pb dating of zircon with a 15 micrometer spatial resolution using NanoSIMS. Gondwana Research, 14, 587-596.

Tatsumoto, M., Nunes, P.D., Knight, R.J., Hedge, C.E., and Unruh, D.M. (1973) U-Th-Pb, Rb-Sr, and K measurements of two Apollo 17 samples. Eos, Transactions, American Geophysical Union, 54, 614-615.

Tera, F., Papanastassiou, D.A., and Wasserburg, G.J. (1974) Isotopic evidence for a terminal lunar cataclysm. Earth and Planetary Science Letters, 22, 1-21.

Terada, K., Saiki, T., Oka, Y., Hayasaka, Y., and Sano, Y. (2005) Ion microprobe U-Pb dating of phosphates in lunar basaltic breccia, elephant moraine 87521. Geophysical Research Letters, 32, L20202, doi:10.1029/2005GL023909.

Terada, K., Anand, M., Sokol, A.K., Bischoff, A., and Sano, Y. (2007a) Cryptomare magmatism 4.35 Gyr ago recorded in lunar meteorite Kalahari 009. Nature, 450, 849-853.

Terada, K., Sasaki, Y., Anand, M., Joy, K.H., and Sano, Y. (2007b) Uranium-lead systematics of phosphates in lunar basaltic regolith breccia, Meteorite Hills 01210. Earth and Planetary Science Letters, 259, 77-84.

Turner, G. (1970) Argon-40/argon-39 dating of lunar rock samples. Apollo 11 Lunar Science Conference, 1665-1684.

Wang, Y., Hsu, W., Guan, Y., Li, X., Li, Q., Liu, Y., and Tang, G. (2012) Petrogenesis of the Northwest Africa 4734 basaltic lunar meteorite. Geochimica et Cosmochimica Acta, 92, 329-344.

Williams, I.S. (1998) U-Th-Pb geochronology by ion microprobe. Reviews in Economic Geology, 7, 1-35.

Wingate, M.T.D., and Compston, W. (2000). Crystal orientation effects during ion microprobe U-Pb analysis of baddeleyite. Chemical Geology, 168, 75-97.

Wingate, M.T.D., Campbell, I.H., Compston, W., Gibson, G.M. (1998) Ion microprobe U-Pb ages for Neoproterozoic basaltic magmatism in south-central Australia and implications for the breakup of Rodinia. Precambrian Research, 87, 135-159.

Yang, W., Lin, Y.T., Zhang, J.C., Hao, J.L., Shen, W.J., and Hu, S., (2012) Precise micrometre-sized Pb-Pb and U-Pb dating with NanoSIMS. Journal of Analytical Atomic Spectrometry, 27, 479-487.

Zhang, A.C., Hsu, W.B., Li, Q.L., Liu, Y., Jiang, Y., and Tang, G.Q. (2010) SIMS Pb/Pb dating of Zr-rich minerals in lunar meteorites Miller Range 05035 and LaPaz Icefield

02224: Implications for the petrogenesis of mare basalt. Science China Earth Sciences, 53, 327-334.

Figure captions

Figure 1. Chemical composition of tranquillityite in Apollo 11 and 17 high-Ti mare basalts 10044, 75055 and 74255, plotted in a ternary diagram TiO_2-SiO_2-ZrO_2. Data for lunar tranquillityite in basalts collected during the Apollo 11, 12 and 17 missions, as well as for terrestrial tranquillityite have been plotted for comparisons (data sources same as given in Table 1).

Figure 2. Secondary electron image of a sputtered crater produced in tranquillityite by a 30 minutes analysis. Abbreviations are bdy: baddeleyite and trq: tranquillityite.

Figure 3. Secondary ion images of ^{47}Ti, ^{91}Zr, ^{206}Pb and $^{238}U^{16}O$ on the area enclosing tranquillityite #14 and an associated baddeleyite grain in sample 10044 (data processed with the L'Image software package, L.R. Nittler, Carnegie Institution, USA). UO intensity is higher and ^{206}Pb intensity is lower in baddeleyite compared to tranquillityite. This is related to the better Pb ionization efficiency in tranquillityite compared to baddeleyite.

Figure 4. $^{207}Pb/^{206}Pb$ vs. $^{204}Pb/^{206}Pb$ diagram and weighted mean $^{207}Pb/^{206}Pb$ dates calculated for tranquillityites in high-Ti mare basalts 10044, 75055 and 74255. In the right panels, data are plotted in the same order as in Table 2. No common Pb correction has been applied to the data (see text for details). The thick grey curves on extreme right are the probability distribution curves of the $^{207}Pb/^{206}Pb$ dates. The two light grey analyses for samples 74255 have been excluded from date calculation. In $^{207}Pb/^{206}Pb$ vs. $^{204}Pb/^{206}Pb$ diagrams,

uncertainties are portrayed at the 1σ level, whereas uncertainty bars in the weighted mean date diagrams are at the 2σ level.

Figure 5. Synthesis of the crystallization ages of the different types of high-Ti Apollo 11 and 17 mare-basalts. Rb-Sr (squares), Sm-Nd (circles) and Pb/Pb (diamonds) ages displayed in the figure are compiled in Table 3, where references are given. The blue stars represent previously estimated crystallization ages of different types of Apollo 11 and 17 units (see Stöffler and Ryder 2001, and references therein). All error bars represent the 2σ uncertainties associated with dates. Dates displayed next to each group correspond to the weighted average of individual dates, and are interpreted as crystallization ages of each group.

Figure 6. La (ppm) vs. K (ppm) diagram showing the composition of the samples from the different types of high-Ti Apollo 11 and 17 mare basalts included in the age synthesis (data have been compiled from the Lunar Sample Compendium - http://curator.jsc.nasa.gov/lunar/compendium.cfm).

This is a preprint, the final version is subject to change, of the American Mineralogist (MSA)
Cite as Authors (Year) Title. American Mineralogist, in press.
(DOI will not work until issue is live.) DOI: http://dx.doi.org/10.2138/am.2014.4467

Table 1. Representative chemical compositions of lunar and terrestrial tranquillityites.

Oxide	10044		75055		74255		Apollo 11*		Apollo 11†		Apollo 12*		Apollo 12‡		Apollo 17§		Terrestrial‖	
	n = 10		n = 10		n = 3		n = 7		n = 15		n = 6		n = 2		n = 3		n = 4	
	wt.%	sd	wt.%	sd	1.9	0.5	wt.%	sd	wt.%	sd	wt.%	sd	wt.%	sd	wt.%	sd	wt.%	sd
SiO_2	14.1	0.5	14.7	0.5	16.0	0.6	14.2	1.2	15.0	0.4	14.2	1.1	14.7	1.0	14.0	0.7	16.6	1.5
TiO_2	20.3	2.1	21.8	1.9	21.3	0.7	19.8	0.8	20.4	1.0	18.9	1.5	19.0	0.3	20.8	0.4	23.4	0.8
Al_2O_3	1.0	0.1	1.0	0.4	1.9	0.5	0.8	0.1	1.1	0.6	1.4	0.4	4.8	0.4	1.0	0.2	0.9	0.6
FeO	43.0	1.2	43.9	1.2	41.1	2.4	42.4	0.7	42.7	0.6	42.3	0.6	39.9	2.8	41.5	0.8	44.7	1.0
CaO	1.2	0.3	1.4	1.0	1.3	0.2	1.1	0.1	1.1	0.1	1.4	0.2	1.9	0.4	0.9	0.1	1.4	0.2
ZrO_2	16.4	2.1	15.3	0.9	16.4	0.3	16.8	0.6	14.2	1.3	17.3	0.6	19.5	4.9	17.2	1.2	9.2	1.7
HfO_2	0.4	0.4	0.7	0.6	0.5	0.3	0.1	0.2	0.3	0.0	0.3	0.4	-	-	0.2	0.0	0.1	0.0
Y_2O_3	2.7	1.4	2.3	0.7	2.2	0.3	3.0	0.9	2.5	0.4	2.8	1.8	-	-	3.1	0.4	0.6	0.5
Nb_2O_5	0.9	0.5	1.0	0.5	0.6	0.4	-	-	0.7	0.2	0.3	-	-	-	0.7	0.1	0.2	0.1

Note: Data are from Lovering et al. (1971)*, Rasmussen et al. (2008)†, Simpson and Bowie (1971)‡, Meyer and Boctor (1974)§ and Rasmussen et al. (2012)‖.

Table 2. NanoSIMS Pb/Pb data for analyses carried out in high-Ti mare basalts 10044, 75055 and 74255.

Analysis	$^{204}Pb/^{206}Pb$	1σ (%)	$^{207}Pb/^{206}Pb$	1σ (%)	f_{206} (%)†	$^{207}Pb/^{206}Pb$ age (Ma)	1σ (Ma)
Trq5#1	0.00007	36	0.3493	0.7	0.12	3704	11
Trq10#1	0.00010	38	0.3601	0.9	0.15	3750	13
Trq10#2	0.00018	41	0.3567	1.2	0.28	3736	19
Trq8#1	0.00010	33	0.3549	0.7	0.16	3728	11
Trq8#2	0.00014	33	0.3551	0.9	0.22	3729	14
Trq11#5	0.00010	28	0.3505	0.7	0.17	3709	10
Trq11#3	0.00013	30	0.3525	0.8	0.21	3718	12
Trq11#4	0.00004	58	0.3542	0.9	0.07	3725	13
Trq14#1	0.00013	32	0.3531	0.9	0.21	3720	13
Bad14#2	0.00034	71	0.3444	3.0	0.54	3682	45
Trq34#1	0.00012	100	0.3545	2.5	0.19	3726	38
Trq34#2	0.00018	58	0.3614	1.8	0.28	3756	26
Trq34#3	0.00006	32	0.3606	0.6	0.10	3752	9
Trq33#1	0.00006	26	0.3672	0.5	0.10	3780	7
Trq33#2	0.00005	33	0.3662	0.5	0.07	3776	8
Trq33#3	0.00017	35	0.3687	1.0	0.26	3786	16
Trq33#4	0.00008	38	0.3651	0.8	0.13	3771	12
Trq23#3	0.00007	24	0.3668	0.5	0.12	3778	7
Trq24#1	0.00004	100	0.3758	1.5	0.07	3815	22
Trq17#1	0.00000	50	0.3637	0.6	0.00	3765	10
Trq17#2	0.00007	41	0.3692	0.8	0.11	3788	12
Trq17#3	0.00002	55	0.3608	0.5	0.03	3753	8
Trq7#3	0.00007	19	0.3543	0.4	0.11	3726	6
Trq7#2	0.00009	19	0.3572	0.4	0.14	3738	6
Trq7#1	0.00008	33	0.3590	0.7	0.13	3746	10
Trq4#1‡	0.00009	32	0.3665	0.7	0.14	3777	10
Trq4#2	0.00004	21	0.3583	0.3	0.06	3743	4
Trq9#2	0.00002	35	0.3589	0.4	0.04	3745	6
Trq18#1‡	0.00003	54	0.3488	0.7	0.05	3702	11

†f_{206} denotes the unradiogenic fraction of ^{206}Pb, calculated using the measured $^{204}Pb/^{206}Pb$ ratios and the Broken Hill galena Pb isotope composition reported by Sangster et al. (2000) (see text for details).

‡Analyses excluded from date calculations.

Table 3. A compilation of previous age determinations carried out on Apollo 11 and 17 high-Ti mare basalts.

Sample	Type	Age (Ma)	2σ (Ma)	Method	References
10017	A	3576	56	Rb-Sr	Papanastassiou et al. (1970)
10024	A	3595	110	Rb-Sr	Papanastassiou and Wasserburg (1971)
10057	A	3610	73	Rb-Sr	Papanastassiou et al. (1970)
10069	A	3656	99	Rb-Sr	Papanastassiou et al. (1970)
10071	A	3662	63	Rb-Sr	Papanastassiou et al. (1970)
10072	A	3642	60	Rb-Sr	Papanastassiou et al. (1977)
		3575	27	Sm-Nd	Papanastassiou et al. (1977)
10058	B1	3715	110	Rb-Sr	Papanastassiou et al. (1970)
		3616	220	Rb-Sr	Snyder et al. (1994)
		3697	110	Sm-Nd	Snyder et al. (1994)
10044	B1	3694	68	Rb-Sr	Papanastassiou et al. (1970)
		3713	8	Pb/Pb	This study
10047	B1	3709.5	4.2	Pb/Pb	Rasmussen et al. (2008)
10062	B2	3911	140	Rb-Sr	Papanastassiou et al. (1977)
		3883	100	Sm-Nd	Papanastassiou et al. (1977)
10003	B2	3779	110	Rb-Sr	Papanastassiou and Wasserburg (1975)
70135	A	3825	73	Rb-Sr	Nyquist et al. (1975)
		3770	60	Sm-Nd	Nyquist et al. (1979)
71539	A	3733	110	Rb-Sr	Paces et al. (1991)
		3744	67	Sm-Nd	Paces et al. (1991)
75035	A	3808	130	Rb-Sr	Murthy and Coscio (1976)
75055	A	3752	60	Rb-Sr	Tera et al. (1974)
		3769	8	Pb/Pb	This study
75075	B	3809	120	Rb-Sr	Murthy and Coscio (1976)
		3839	91	Rb-Sr	Nyquist et al. (1975)
		3827	73	Rb-Sr	Combined datasets
		3709	65	Sm-Nd	Lugmair et al. (1975)
70139	B	3713	120	Rb-Sr	Paces et al. (1991)
		3710	120	Sm-Nd	Paces et al. (1991)
70035	B	3790	190	Rb-Sr	Evensen et al. (1973)
		3726	110	Rb-Sr	Nyquist et al. (1974)
		3734	93	Rb-Sr	Combined datasets
70017	B	3746	210	Rb-Sr	Nyquist et al. (1975)
74255	C	3751	77	Rb-Sr	Nyquist et al. (1976)
		3694	140	Rb-Sr	Murthy and Coscio (1976)
		3750	120	Rb-Sr	Combined datasets
74275	C	3829	140	Rb-Sr	Murthy and Coscio (1977)
		3736	10	Pb/Pb	This study

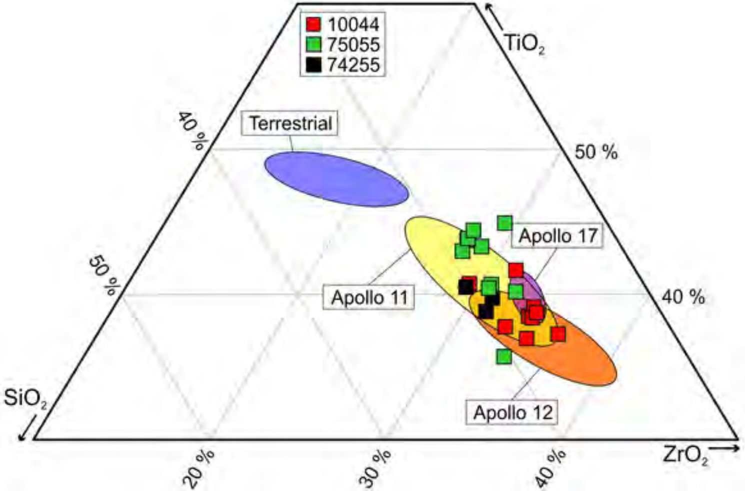
10044
75055
74255
TiO2
Terrestrial
40 %
50 %
Apollo 17
50 %
Apollo 11
40 %
SiO2
Apollo 12
20 %
30 %
40 %
ZrO2

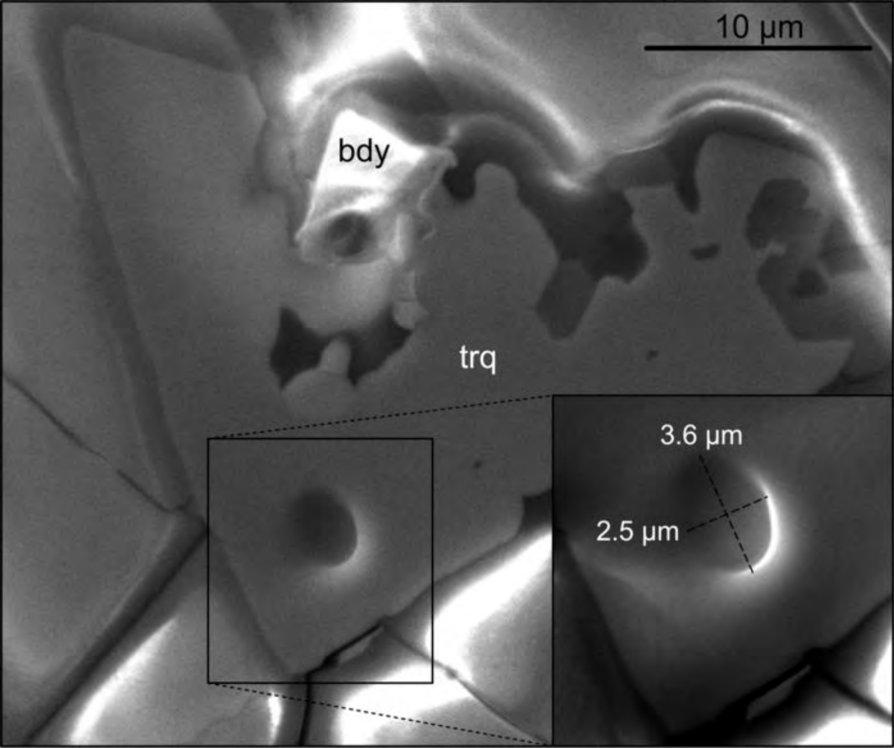
10 μm
bdy
trq
3.6 μm
2.5 μm

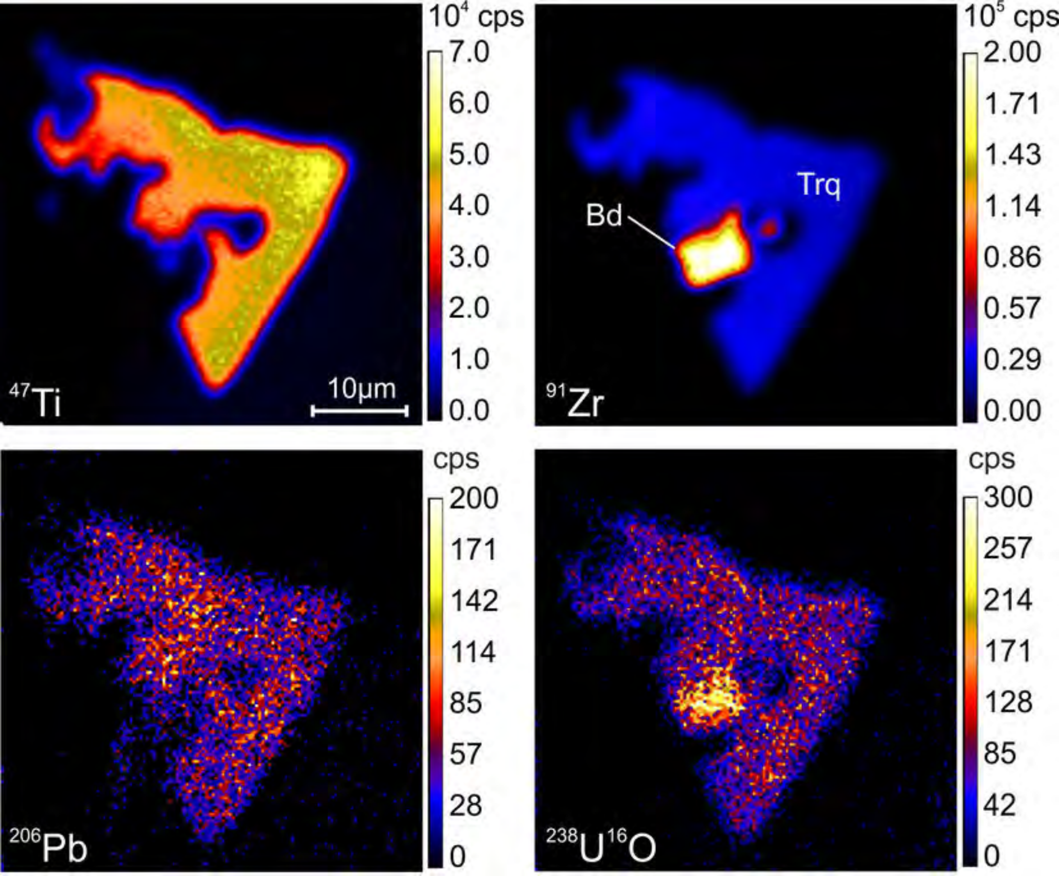

10^4 cps
7.0
6.0
5.0
4.0
3.0
2.0
1.0
0.0
10μm
47Ti
10^5 cps
2.00
1.71
1.43
1.14
0.86
0.57
0.29
0.00
Trq
Bd
91Zr
cps
200
171
142
114
85
57
28
0
206Pb
cps
300
257
214
171
128
85
42
0
238U16O

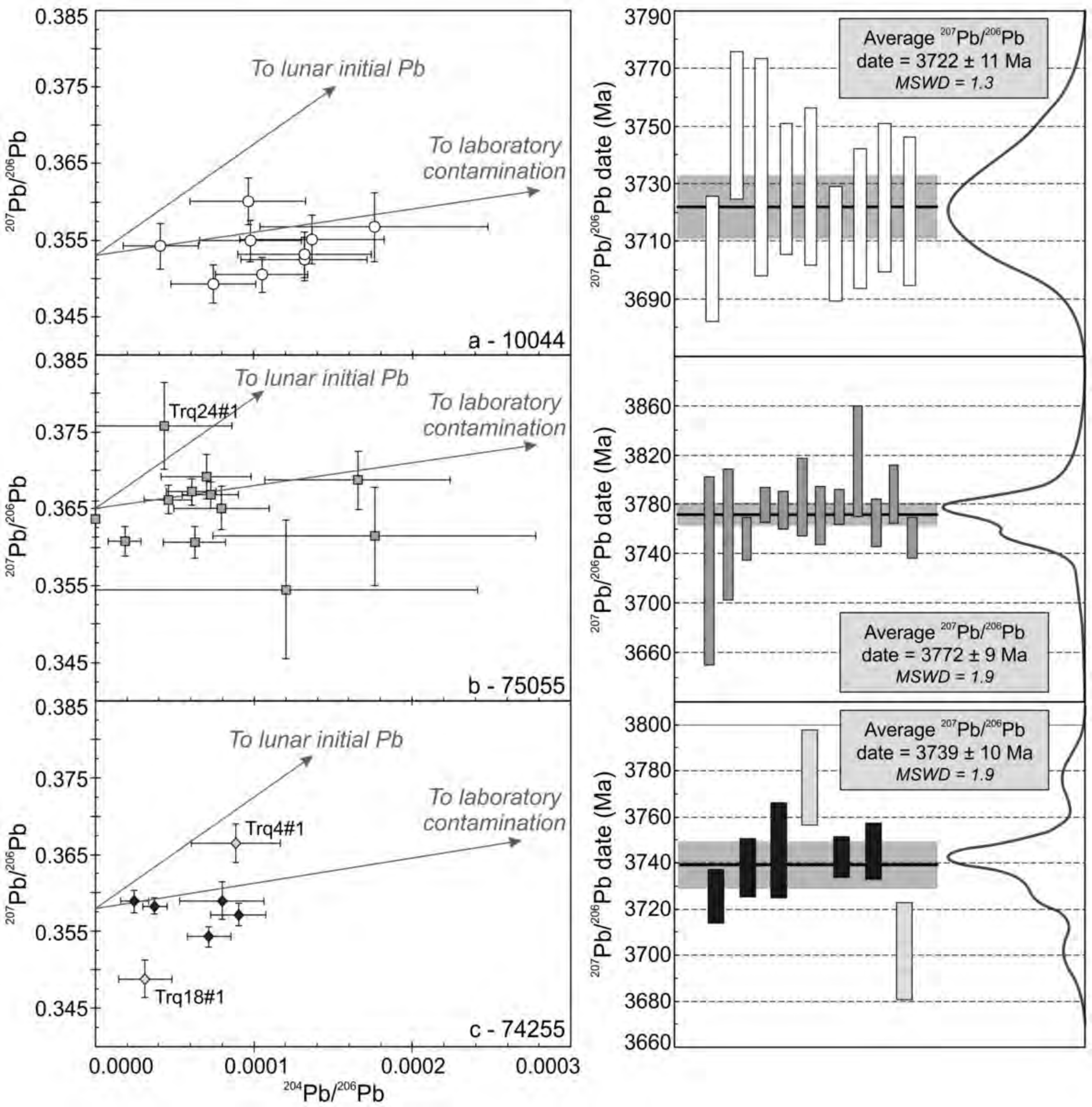
To lunar initial Pb
To laboratory contamination
a - 10044
b - 75055
c - 74255
Trq24#1
Trq4#1
Trq18#1
$^{207}Pb/^{206}Pb$
$^{204}Pb/^{206}Pb$
$^{207}Pb/^{206}Pb$ date (Ma)
Average $^{207}Pb/^{206}Pb$ date = 3722 ± 11 Ma
MSWD = 1.3
Average $^{207}Pb/^{206}Pb$ date = 3772 ± 9 Ma
MSWD = 1.9
Average $^{207}Pb/^{206}Pb$ date = 3739 ± 10 Ma
MSWD = 1.9

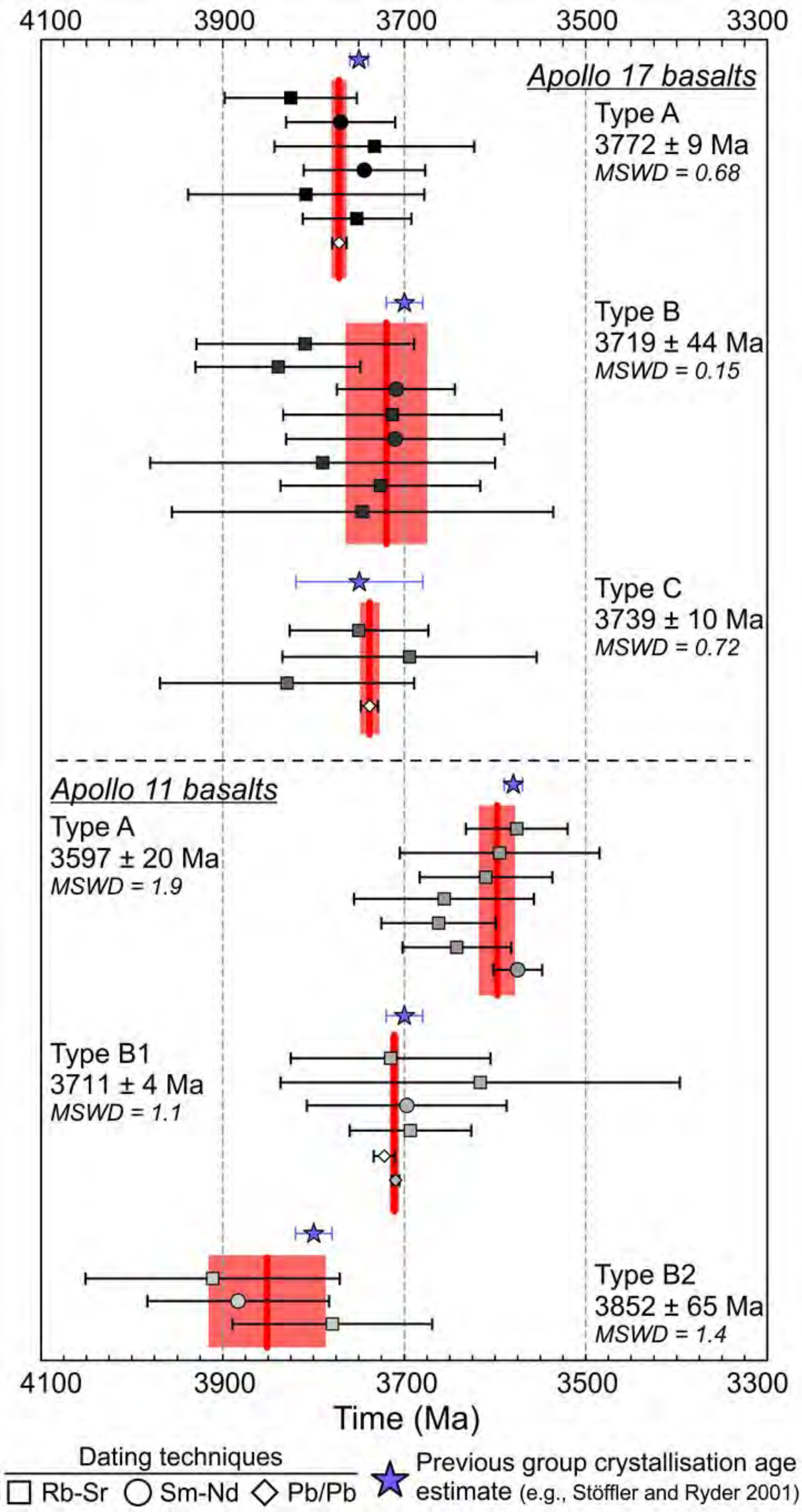
4100
3900
3700
3500
3300
Apollo 17 basalts
Type A
3772 ± 9 Ma
MSWD = 0.68
Type B
3719 ± 44 Ma
MSWD = 0.15
Type C
3739 ± 10 Ma
MSWD = 0.72
Apollo 11 basalts
Type A
3597 ± 20 Ma
MSWD = 1.9
Type B1
3711 ± 4 Ma
MSWD = 1.1
Type B2
3852 ± 65 Ma
MSWD = 1.4
Time (Ma)
Dating techniques
Rb-Sr
Sm-Nd
Pb/Pb
Previous group crystallisation age estimate (e.g., Stöffler and Ryder 2001)

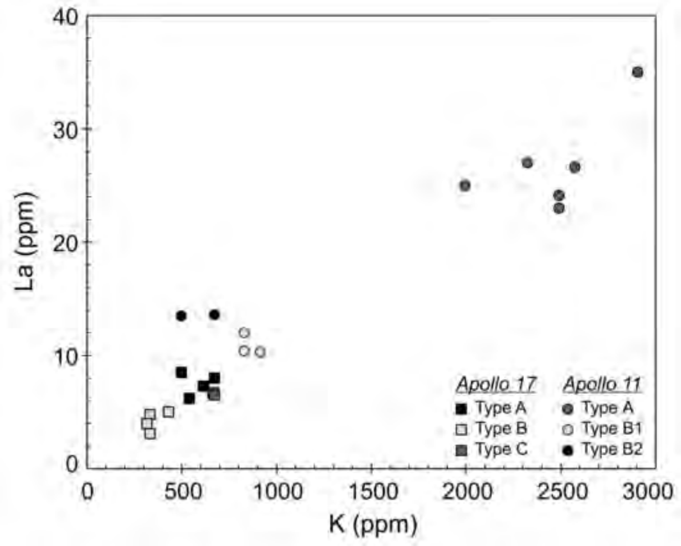

40
30
20
10
0
La (ppm)
0
500
1000
1500
2000
2500
3000
K (ppm)
Apollo 17
Type A
Type B
Type C
Apollo 11
Type A
Type B1
Type B2